



Relationships between Pacific and Atlantic ocean sea surface temperatures and U.S. streamflow variability

Glenn A. Tootle¹ and Thomas C. Piechota²

Received 13 April 2005; revised 8 March 2006; accepted 23 March 2006; published 19 July 2006.

[1] An evaluation of Pacific and Atlantic Ocean sea surface temperatures (SSTs) and continental U.S. streamflow was performed to identify coupled regions of SST and continental U.S. streamflow variability. Both SSTs and streamflow displayed temporal variability when applying the singular value decomposition (SVD) statistical method. Initially, an extended temporal evaluation was performed using the entire period of record (i.e., all years from 1951 to 2002). This was followed by an interdecadal-temporal evaluation for the Pacific (Atlantic) Ocean based on the phase of the Pacific Decadal Oscillation (PDO) (Atlantic Multidecadal Oscillation (AMO)). Finally, an extended temporal evaluation was performed using detrended SST and streamflow data. A lead time approach was assessed in which the previous year's spring-summer season Pacific Ocean (Atlantic Ocean) SSTs were evaluated with the current water year continental U.S. streamflow. During the cold phase of the PDO, Pacific Ocean SSTs influenced streamflow regions (southeast, northwest, southwest, and northeast United States) most often associated with El Niño–Southern Oscillation (ENSO), while during the warm phase of the PDO, Pacific Ocean SSTs influenced non-ENSO streamflow regions (Upper Colorado River basin and middle Atlantic United States). ENSO and the PDO were identified by the Pacific Ocean SST SVD first temporal expansion series as climatic influences for the PDO cold phase, PDO warm phase, and the all years analysis. Additionally, the phase of the AMO resulted in continental U.S. streamflow variability when evaluating Atlantic Ocean SSTs. During the cold phase of the AMO, Atlantic Ocean SSTs influenced middle Atlantic and central U.S. streamflow, while during the warm phase of the AMO, Atlantic Ocean SSTs influenced upper Mississippi River basin, peninsular Florida, and northwest U.S. streamflow. The AMO signal was identified in the Atlantic Ocean SST SVD first temporal expansion series. Applying SVD, first temporal expansions series were developed for Pacific and Atlantic Ocean SSTs and continental U.S. streamflow. The first temporal expansion series of SSTs and streamflow were strongly correlated, which could result in improved streamflow predictability.

Citation: Tootle, G. A., and T. C. Piechota (2006), Relationships between Pacific and Atlantic ocean sea surface temperatures and U.S. streamflow variability, *Water Resour. Res.*, 42, W07411, doi:10.1029/2005WR004184.

1. Introduction

[2] Sea surface temperature (SST) variability can provide important predictive information about hydrologic variability in regions around the world. While coupled SST variability and continental U.S. precipitation (and drought) variability has been examined, water managers could benefit from an evaluation of coupled SST variability and continental U.S. streamflow variability, focusing on improving long lead time forecasts of streamflow. Continental U.S. streamflow regions have been identified that respond to oceanic/atmospheric phenomena such as the El Niño–Southern Oscillation (ENSO) [e.g., *Cayan and Peterson,*

1989; *Cayan and Webb,* 1992; *Kahya and Dracup,* 1993, 1994a, 1994b; *Maurer et al.,* 2004], the Pacific Decadal Oscillation (PDO) [e.g., *Maurer et al.,* 2004], and the Atlantic Multidecadal Oscillation (AMO) [e.g., *Enfield et al.,* 2001; *Rogers and Coleman,* 2003]. While the interannual ENSO experiences a 2–7 year periodicity [*Philander,* 1990], the interdecadal PDO [*Mantua et al.,* 1997; *Mantua and Hare,* 2002] and AMO [*Kerr,* 2000; *Gray et al.,* 2004] exhibit long-term (e.g., 25–30 year) periodicity of warm and cold phases. Although each of these oceanic/atmospheric phenomena represent SST variability, the SST variability represented is for a specific, spatially predetermined region (e.g., tropical Pacific Ocean, northern Pacific Ocean, northern Atlantic Ocean). The utilization of SSTs for entire regions (Pacific and Atlantic Oceans) eliminates any spatial bias as to which oceanic SST region (or regions) impact continental U.S. streamflow. This could result in new SST (and continental U.S. streamflow) regions being identified as having coupled impacts. Additionally,

¹Department of Civil and Architectural Engineering, University of Wyoming, Laramie, Wyoming, USA.

²Department of Civil and Environmental Engineering, University of Nevada, Las Vegas, Nevada, USA.

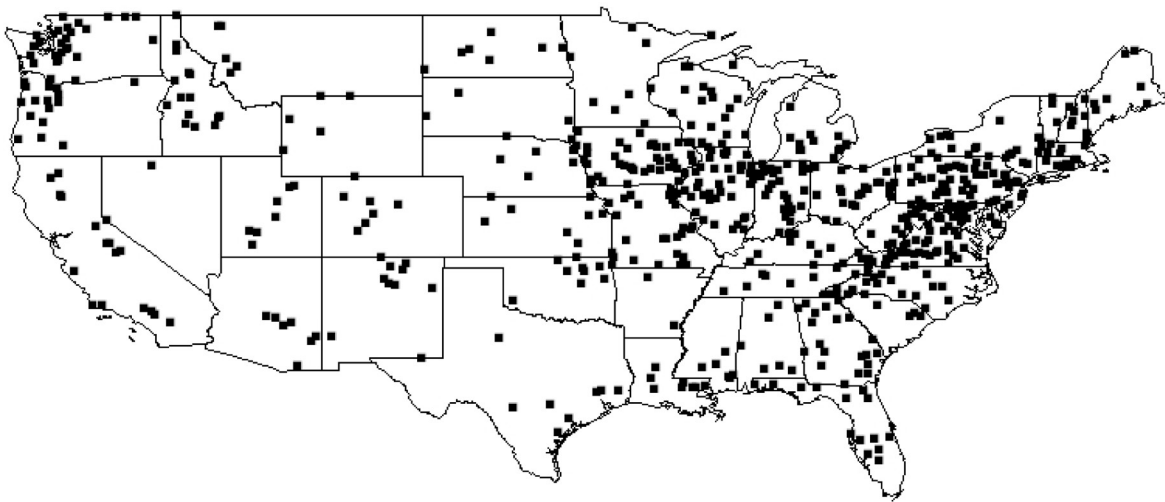


Figure 1. Locations of unimpaired U.S. Geological Survey streamflow stations in the continental United States (1951–2002).

when evaluating SSTs for extended time series, both interdecadal and interannual SST oscillations can be considered.

[3] Various methods, including canonical correlation analysis, combined principal component analysis and singular value decomposition (SVD) are available to determine coupled relationships between two, spatial-temporal fields such as SSTs and climatic variables. *Bretherton et al.* [1992] evaluated several statistical methods designed to determine coupled relationships between two, spatial-temporal fields and concluded SVD was simple to perform and preferable for general use. *Wallace et al.* [1992] evaluated the interannual coupling of wintertime Pacific SSTs and atmospheric 500-mbar height and determined that, when compared to other techniques, SVD isolates the most important modes of variability.

[4] SVD has also been used to identify coupled relationships between oceanic SST variability and hydrologic variability in regions outside the continental United States. *Uvo et al.* [1998] applied SVD to evaluate Pacific and Atlantic Ocean SSTs and northeast Brazilian precipitation. The Pacific and Atlantic Oceans were evaluated independently using both a simultaneous and lagged approach. In each case, the majority of variability was explained by the first mode of SVD [*Uvo et al.*, 1998]. *Rodriguez-Fonseca and de Castro* [2002] utilized a lag approach when applying SVD to evaluate Atlantic Ocean SSTs and Iberian/northwest African precipitation. Applying SVD, *Shabbar and Skinner* [2004] utilized a lag approach in which winter global SSTs and summer Canadian drought (e.g., Palmer Drought Severity Index (PDSI) values) were evaluated. The first three modes of SVD explained approximately 80% of the variance with each mode representing a distinct oceanic/atmospheric phenomena (e.g., first mode, AMO; second mode, ENSO; third mode, PDO) [*Shabbar and Skinner*, 2004].

[5] In the continental United States, SVD has been utilized to evaluate coupled oceanic SST variability and U.S. precipitation (and drought) variability. *Wang and Ting* [2000] evaluated Pacific Ocean SSTs and continental U.S. precipitation for concurrent (overlapping) time periods and identified simultaneous patterns of SST influence on precipitation. *Rajagopalan et al.* [2000] utilized SVD and

applied a lag approach to evaluate global SST impacts on continental U.S. drought (PDSI). The SST regions identified in each of these studies included a tropical Pacific Ocean region (interannual) and a north central Pacific Ocean region, and a precipitation (drought) region in the southwest United States.

[6] The goal of the research presented here is to identify coupled regions of SST variability and continental U.S. hydrologic variability by utilizing an improved long-term streamflow data set. The use of streamflow as the hydrologic variable is important since streamflow acts as an integrator of the various components of the hydrologic cycle (e.g., precipitation, infiltration, evapotranspiration). Furthermore, an extended continental U.S. streamflow data set allows for the evaluation of interdecadal influences. By performing an extended temporal evaluation of SSTs and streamflow, interannual and interdecadal variations may be integrated and thus provide improved predictors for long-range streamflow forecasting.

2. Data

[7] The major data sets used to develop the relationships between continental U.S. streamflow and oceanic SST variability were unimpaired streamflow data for the continental United States and oceanic SST data for the Pacific and Atlantic Oceans.

2.1. Streamflow Data

[8] Unimpaired streamflow stations (1,009) were identified from *Wallis et al.* [1991] and, utilizing the U.S. Geological Survey (USGS) NWISWeb Data retrieval (<http://waterdata.usgs.gov/nwis/>), the period of record was extended from 1988 to 2002. This resulted in 639 stations having monthly flowrate data for the period from 1951 to 2002 (Figure 1). The reduction of 370 (1009 minus 639) unimpaired streamflow stations was a result of the data not being updated on the USGS Web site and missing data. A review of the USGS NWISWeb resulted in 172 stations not having updated data, 184 stations missing a year (or multiple years) of data and 14 stations missing both updated and a year (or multiple years) of data. However, extending

Table 1. Definition of Cold and Warm Years for the PDO and the AMO

	PDO	AMO
Cold	1950–1976	1964–1994
Warm	1977–2002	1950–1963, 1995–2002

the period of record was important because it provided both recent data and, increased the number of years used when performing the analysis. The average monthly streamflow rates (in cubic feet per second (cfs)) were averaged for the water year (October of the previous year to September of the current year) and converted into streamflow volumes (km^3) with proper conversions. Water year streamflow data covering a period from 1951 to 2002 (52 years) were then used in the following analysis.

2.2. Pacific and Atlantic Ocean Sea Surface Temperature Data

[9] SST data for the Pacific and Atlantic Oceans were obtained from the National Climatic Data Center (<http://www.cdc.noaa.gov/cdc/data.noaa.ersst.html>). The oceanic SST data consists of average monthly values for a 2° by 2° grid cell [Smith and Reynolds, 2002]. The extended reconstructed global SSTs were based on the Comprehensive Ocean-Atmosphere Data Set (COADS) from 1856 to present [Smith and Reynolds, 2002]. A quality control procedure was developed by Smith and Reynolds utilizing a base period (1961–1991) to develop the reconstructed SSTs back to 1854. The uncertainty in the reconstructed data decreases through most of the period (1854 to present) with the smallest uncertainty after 1950 [Smith and Reynolds, 2002]. This reduction in data uncertainty was primarily due to improved aerial coverage of the oceans.

[10] The region of Pacific Ocean SST data used for the analysis was longitude 120°E to longitude 80°W and latitude 20°S to latitude 60°N while the region of Atlantic Ocean SST data used for the analysis was longitude 80°W to longitude 0° and latitude 20°S to latitude 60°N . These regions represent the majority of atmospheric/oceanic influence on U.S. climate (i.e., storm tracks such as Pacific Ocean frontal storms) and were consistent with other studies, including that of Wang and Ting [2000]. The average monthly SSTs were averaged for the spring-summer season (April to September) covering a period from 1950 to 2001 (52 years).

3. Methods

3.1. Temporal Phase Definitions

[11] Initially, an extended temporal evaluation was performed in which SVD was applied to previous spring-summer season Pacific (Atlantic) Ocean SSTs and current water year continental U.S. streamflow for all years of record (referred to as the all years analysis). Next, an interdecadal phase temporal evaluation was performed in which SVD was applied using the cold or warm phase of the PDO (AMO) to evaluate Pacific (Atlantic) Ocean SSTs and current water year continental U.S. streamflow (referred to as the PDO cold years (AMO cold years) and the PDO warm years (AMO warm years) analysis). The PDO (AMO) phase (warm/positive and cold/negative) was defined

according to the sign of the PDO (AMO) index. The PDO (AMO) was selected for the interdecadal phase temporal evaluation due to the longevity (i.e., 25–30 years) of the cold or warm phase and the influence of the PDO (AMO) on continental U.S. hydrology. McCabe *et al.* [2004] evaluated coupled effects of PDO and AMO for four periods: PDO warm/AMO warm (1926–1943), PDO cold and AMO warm (1944–1963), PDO cold and AMO cold (1964–1976), and PDO warm and AMO cold (1977–1994). Mantua [2004] suggested that the PDO shifted from the warm phase to the cold phase around 2000 while recent studies [Enfield *et al.*, 2001; McCabe *et al.*, 2004; Gray *et al.*, 2004] suggest that the AMO returned to a warm phase in 1995. The periods used in the McCabe *et al.* [2004] study were adopted for this study to categorize PDO (or AMO) warm and cold years, for the spring-summer season oceanic SSTs, with the assumption that the PDO remains in the warm phase until the end of the study period (2001) and the AMO shifts to warm in 1995 and remains until the end of the study period (Table 1).

[12] For both the Pacific (Atlantic) Ocean SSTs and continental U.S. streamflow data sets, anomalies were calculated in which the anomaly was defined as the deviation of the seasonal (or water year) mean from the long-term average. The anomalies were then standardized by the standard deviation, and the standardized anomalies for both data sets were used in the following analysis.

[13] The authors acknowledge the short time period (52 years) used in this research to evaluate interdecadal variability. This is the primary limitation of the published studies cited in the Introduction section of this study. While a longer time period would be more appropriate, this is not possible with instrumental records. This problem can be overcome using long-duration reconstructions of climate and streamflow provided by tree rings. While the PDO, AMO, ENSO and global SSTs have been reconstructed, the database of continental U.S. streamflow reconstructions is limited (<http://www.ncdc.noaa.gov/paleo/recons.html>) and, currently, a comprehensive study is not possible.

3.2. Singular Value Decomposition

[14] As previously discussed, singular value decomposition (SVD) is a powerful statistical tool for identifying coupled relationships between two, spatial-temporal fields. Bretherton *et al.* [1992] and Strang [1998] provide a detailed discussion of the theory of SVD. A brief description of SVD, as applied in the current study, is hereby provided. Initially, a matrix of standardized SST anomalies and a matrix of standardized streamflow anomalies were developed. The time dimension of each matrix (i.e., years) must be equal while the spatial component (i.e., number of Pacific (Atlantic) Ocean SST cells or continental U.S. streamflow stations) can vary in dimension. The cross-covariance matrix was then computed for the two spatial, temporal matrices and SVD was applied to the cross-covariance matrix. By utilizing the cross-covariance matrix of the SST and streamflow fields, physical information of the relationship between the two fields can be obtained. Applying SVD allows for the creation of orthogonal bases that diagonalize the cross-covariance matrix, resulting in the new factorization of the cross-covariance matrix (e.g., orthogonal * diagonal * orthogonal) [Strang, 1998]. The resulting decomposition of the cross-covariance matrix

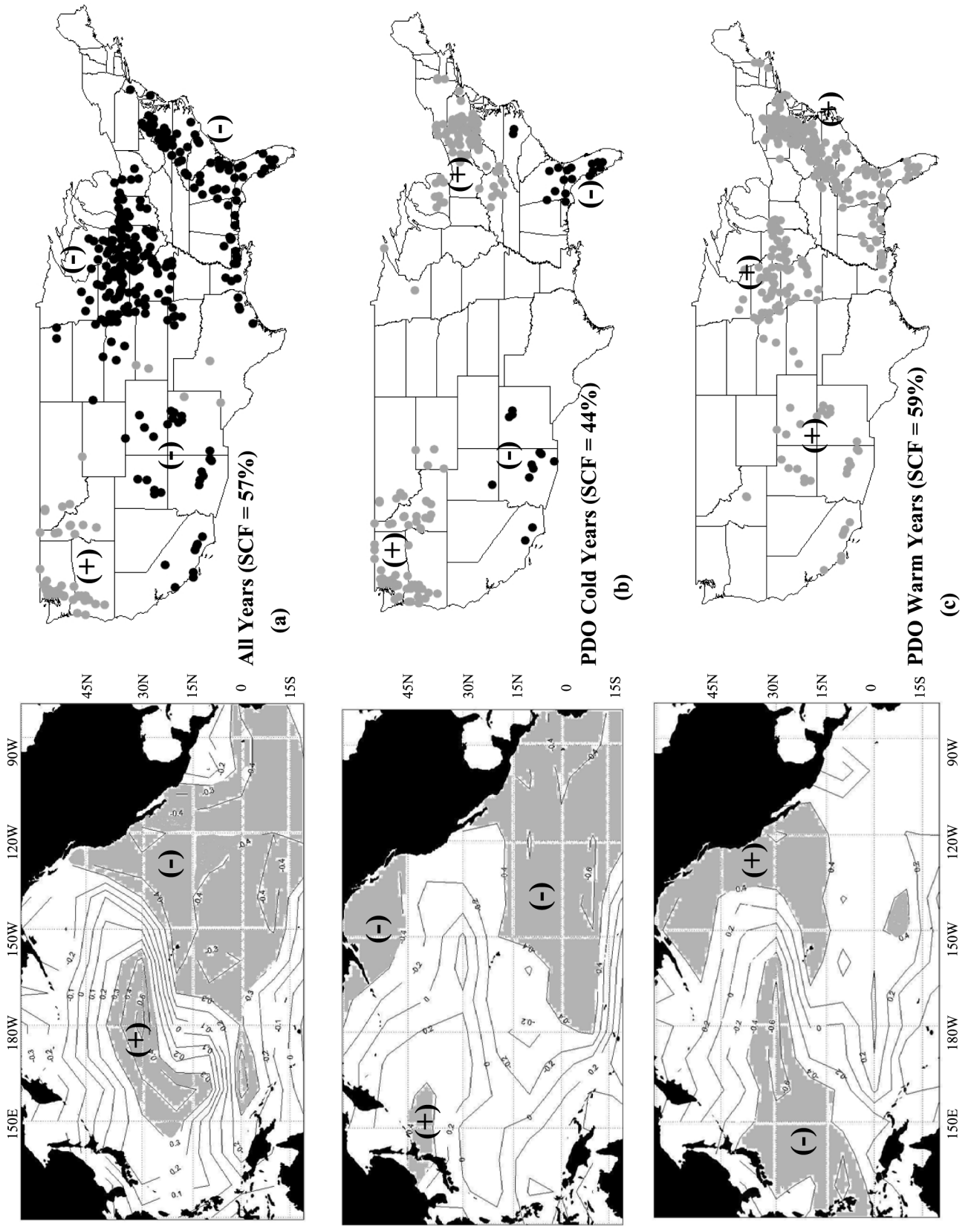


Figure 2

created two matrices of singular vectors and one matrix of singular values. The singular values were ordered such that the first singular value (first mode) was greater than the second singular value and so on. *Bretherton et al.* [1992] defines the squared covariance fraction (SCF) as a useful measurement for comparing the relative importance of modes in the decomposition. Each singular value was squared and divided by the sum of all the squared singular values to produce a fraction (or percentage) of squared covariance for each mode. Additionally, *Wallace et al.* [1992] and *Bretherton et al.* [1992] define the normalized square covariance (NSC) as

$$\frac{\|C\|_F^2}{N_s * N_z}$$

where $\|C\|_F^2$ is the sum of the squares of the singular values and N_s is the number of SST data points and N_z is the number of streamflow stations.

[15] Finally, the two matrices of singular vectors were examined, generally referred to as the left (i.e., SSTs) matrix and the right (i.e., streamflow) matrix. The first column of the left matrix (first mode) was projected onto the standardized SST anomalies matrix, and the first column of the right matrix (first mode) was projected onto the standardized streamflow anomalies matrix. This resulted in the first temporal expansion series of the left and right fields, respectively. The left heterogeneous correlation figure (for the first mode) was determined by correlating the SST values of the left matrix with first temporal expansion series of the right field and the right heterogeneous correlation figure (for the first mode) was determined by correlating the streamflow values of the right matrix with the first temporal expansion series of the left field. Utilizing the approach of *Rajagopalan et al.* [2000] and *Uvo et al.* [1998], heterogeneous correlation figures displaying significant (95%) correlation values (Pearson product moment coefficient of correlation) for SST regions and streamflow regions were reported for Pacific Ocean all years, PDO cold years, PDO warm years, Atlantic Ocean all years, AMO cold years and AMO warm years. Additionally, SVD was applied to detrended SST and streamflow data for Pacific Ocean all years and Atlantic Ocean all years. The detrending was based on the least squares fit of a straight (or composite) line to the data sets and subtracting the resulting function from the data. Detrending the SST and streamflow data removes any trends in the data sets that may bias the analysis and mask the underlying variability. For the analysis, autocorrelation was also investigated and, based on the results, did not significantly impact the SST and streamflow regions identified in the heterogeneous correlation figures.

[16] While SVD is a powerful tool for the statistical analysis of two spatial, temporal fields, there exist several caveats (or limitations) to its use that should be investigated [*Newman and Sardeshmukh*, 1995]. Generally, if the leading (first, second or third) modes explain a significant

amount of the variance of the two fields, then SVD can be applied to determine the strength of the coupled variability present [*Newman and Sardeshmukh*, 1995]. However, when using SVD to examine two fields, the examiner must exhibit caution when attempting to explain the physical cause of the results [*Newman and Sardeshmukh*, 1995].

4. Results

[17] The results of the SVD analysis of Pacific (and Atlantic) Ocean SSTs and continental U.S. streamflow are presented this section. Initially, Pacific Ocean SSTs and continental U.S. streamflow were evaluated for the entire period of record (section 4.1.1). This evaluation considers both interdecadal (e.g., PDO warm and cold phases) and interannual (e.g., ENSO warm and cold phases) variability. Next, only cold years of the interdecadal PDO (section 4.1.2) and only warm years of the PDO (section 4.1.3) were examined. Thus interannual (e.g., ENSO warm and cold phases) variability was considered in each analysis. Atlantic Ocean SSTs and continental U.S. streamflow were evaluated for the entire period of record (section 4.2.1), AMO cold years (section 4.2.2) and AMO warm years (section 4.2.3). Finally, detrended Pacific Ocean (and Atlantic Ocean) SSTs and continental U.S. streamflow were evaluated for the entire period of record (i.e., 4.4). The first mode of variability (only) was reported for each category, based on the significant squared covariance fractions reported for the first mode.

4.1. Pacific Ocean SSTs and Continental U.S. Streamflow (First Mode)

4.1.1. All Years

[18] For the all years analysis, Pacific Ocean SSTs and continental U.S. streamflow resulted in squared covariance fractions of 57% for first mode, 13% for second mode, and 13% for third mode and a NSC value of 3.6%.

[19] Figure 2 represents heterogeneous correlation maps ($|r| > 0.29$) displaying significant Pacific Ocean SST (Figure 2, left) and continental U.S. streamflow regions (Figure 2, right) for the first mode of SVD. The Pacific Ocean SST heterogeneous correlation figure (Figure 2a) was determined by correlating the Pacific Ocean SST values with the first temporal expansion series of continental U.S. streamflow, while the continental U.S. streamflow heterogeneous correlation figure (Figure 2a) was determined by correlating the continental U.S. streamflow values with the first temporal expansion series of Pacific Ocean SSTs. For the SST figures, contours were used to represent correlation values. The gray shading approximates the 95% significance level. For the streamflow figures, circles were used to represent the 95% significance level. Circles were used in lieu of contours because of the unequal spatial distribution of the continental U.S. streamflow stations (Figure 1). The gray circles represent positive correlations, while the black circles represent negative correlations. This approach was

Figure 2. Heterogeneous correlation figures for SVD (first mode) for previous year spring-summer season Pacific Ocean SSTs and current water year U.S. streamflow for (a) all years, (b) PDO cold years, and (c) PDO warm years. Significant (>95%) SST regions were approximated by gray shading. Significant (>95%) negative (positive) streamflow stations were represented by black (gray) circles.

used for the all SST and streamflow heterogeneous correlation maps in this study.

[20] Pacific Ocean SST regions (Figure 2a) were identified near the tropical region (minus sign (negative)) and the north central (plus sign (positive)) region. The tropical Pacific Ocean SST region (interannual SST region) represents the larger spatial area. However, the north central Pacific Ocean SST region displayed higher correlation values. While no physical explanation is offered to explain the north central region, *Wang and Ting* [2000] identified a similar pattern (for the first mode) as did *Rajagopalan et al.* [2000]. Additionally, the Australian Bureau of Meteorology (BOM) identified twelve SST regions in the Pacific Ocean. The SST values are the first twelve components of an empirical orthogonal function (EOF) analysis of the Pacific and Indian Ocean SSTs [*Drosowsky and Chambers*, 1998]. While the first mode (SST 1) represents the interannual or tropical PDO, SST 4 is very similar (spatially) to the pattern identified in the north central Pacific Ocean (Figure 2).

[21] The streamflow regions (Figure 2a) identified include the Upper Colorado River (UCR) basin, Gulf of Mexico, middle Atlantic, southwest and central United States. These regions (minus sign) behave similarly to the interannual SST region such that increased (decreased) streamflow occurs when there are increased (decreased) tropical SSTs. A streamflow region (plus sign) of opposite response was identified in the northwest United States. The northwest U.S. streamflow region behaves opposite of the interannual SST region such that increased (decreased) streamflow occurs when there are decreased (increased) SSTs. It is noteworthy that additional (streamflow) regions (UCR basin, Gulf of Mexico, middle Atlantic and central United States) were identified when compared to the (precipitation) regions (southwest and northwest United States) identified in *Wang and Ting* [2000]. This may be a result of the lead time approach utilized.

[22] While the interannual or tropical PDO SST region was identified as the spatially dominant Pacific Ocean SST region, the identified streamflow regions in the UCR basin and middle Atlantic United States were not identified as interannual SST influenced streamflow regions in previous studies [e.g., *Kahya and Dracup*, 1993]. Additionally, the central U.S. region represents a lagged response region to the interannual SST region, which was not consistent with *Kahya and Dracup* [1993]. The most likely explanation of the varying results was the *Kahya and Dracup* [1993] study focused on ENSO years (only) while the current research included all years.

[23] When utilizing Pacific Ocean SSTs, the results represent a streamflow response to Pacific Ocean SSTs as a whole and were not limited to only interannual influences. The streamflow regions identified appear to represent the combined influences of interannual and interdecadal phenomena. The identification of interannual and interdecadal influenced streamflow regions was further verified when correlating the Pacific Ocean SST SVD first temporal expansion series with the Nino 3.4 [*Trenberth*, 1997] and the unsmoothed PDO [*Mantua et al.*, 1997] indices for the same year and season. Correlation ($|r|$) values were 0.78 (Nino 3.4 index and Pacific Ocean SST SVD first temporal expansion series) and 0.84 (PDO index and Pacific Ocean SST SVD first temporal expansion series), thus showing

that the Pacific Ocean SST SVD first temporal expansion series does relate to both ENSO and PDO signals. *Hidalgo and Dracup* [2001] evaluated spring-summer streamflow and rainfall and acknowledged a possible ENSO – PDO modulation of cold season precipitation in the northern Rocky Mountains while *Nigam et al.* [1999] linked the PDO to the upper/middle Mississippi River (central region) basin. To further evaluate the influence of the interdecadal PDO, the temporal phase (cold and warm) was examined in the following sections.

[24] While the all years analysis above evaluated Pacific Ocean SSTs and continental U.S. streamflow for the entire 52 years of record, an additional analysis was performed using neutral ENSO years as defined by *Tootle et al.* [2005]. As expected, the first mode identified the PDO as the dominate influence while ENSO was a lesser influence.

4.1.2. PDO Cold Years

[25] For the cold years analysis, Pacific Ocean SSTs and continental U.S. streamflow resulted in squared covariance fractions of 44% for first mode, 21% for second mode, and 8% for third mode. When evaluating PDO cold years, Pacific Ocean SSTs and continental U.S. streamflow regions ($|r| > 0.38$) display large differences in the spatial patterns when compared to the all years results. The previously identified ENSO SST region (minus sign) was again significant (Figure 2b), however, the PDO cold years phase appears to reduce and concentrate (spatially) the ENSO SST region along the equator. Additionally, the previously defined north central Pacific SST region (plus sign) was significantly smaller (spatially) and has shifted toward the northwest Pacific Ocean. Finally, a new Pacific Ocean SST region (minus sign) was identified near the western coast of Canada and Alaska.

[26] The most interesting results occurred in the streamflow figure (Figure 2b). The PDO cold, by spatially concentrating the tropical Pacific Ocean SST region (interannual SST region), results in streamflow regions most often associated with the interannual Pacific Ocean SST phenomenon. The northwest U.S. region (plus sign) remained almost unchanged when compared to the all years figure (Figure 2a), with the exception of several significant stations being identified in Wyoming. However, the UCR basin, middle Atlantic and central U.S. regions were no longer significant. Florida and southeast Georgia were the only significant regions remaining in the southeast United States when compared to the all years results. A new streamflow region (plus sign) was identified in the northeast United States not previously identified in the all years figure (Figure 2a). The northeast and northwest U.S. streamflow regions respond to Pacific Ocean SSTs in the same manner (i.e., both streamflow regions have a plus sign). This behavior was consistent with the findings of *Kahya and Dracup* [1993] who identified that the northeast and northwest continental U.S. streamflow regions respond to ENSO similarly. Perhaps during a PDO cold phase, the colder northern Pacific Ocean waters “push” the tropical Pacific Ocean SST belt (i.e., interannual SST region) south such that it is more concentrated, and thus the influence on continental U.S. streamflow is more consistent with past research [e.g., *Kahya and Dracup*, 1993]. When correlating the Pacific Ocean SST SVD first temporal expansion series with the Nino 3.4 and PDO indices for PDO cold years, the

$|r|$ values were 0.93 and 0.73, respectively. When compared to the previously stated $|r|$ values for the all years analysis (0.78 for Nino 3.4 and 0.84 for PDO), the increased strength of the interannual signal was clearly revealed for the PDO cold years.

4.1.3. PDO Warm Years

[27] For the warm years analysis, Pacific Ocean SSTs and continental U.S. streamflow resulted in squared covariance fractions of 59% for first mode, 12% for second mode, and 9% for third mode. When evaluating PDO warm years, Pacific Ocean SSTs and continental U.S. streamflow regions ($|r| > 0.40$) display large differences in the spatial patterns when compared to the all years (and PDO cold years) results. First, a new Pacific Ocean SST region (Figure 2c) was identified near the western coast of the United States and Canada that was significantly correlated with continental U.S. streamflow and the relationship between the tropical Pacific Ocean SST region (interannual SST region) and continental U.S. streamflow has weakened. The weakening of the interannual SST region during the PDO warm years was further verified by correlating the Pacific Ocean SST SVD first temporal expansion series with Nino 3.4 ($|r|$ value of 0.77). Also, the significant SST pattern located over the north central Pacific Ocean was spatially similar when compared to the all years results. While the streamflow regions identified were consistent with the well-established influence of ENSO (e.g., increased (decreased) streamflow in the southwest, central and southeast United States results from increased (decreased) ENSO SSTs), the signs of the Pacific Ocean SST regions (Figure 2c) were opposite when compared to the all years (Figure 2a) and PDO cold years (Figure 2b) figures.

[28] The current (Figure 2c) and the all years (Figure 2a) figures are similar with the exception of the Pacific Northwest region. Additionally, the current (Figure 2c) and previous (Figure 2b) figures result in streamflow being significant in the northwest (coastal Washington/Oregon, Idaho, Montana, and Wyoming) and northeast (western Pennsylvania) continental U.S. during PDO cold years but not significant during PDO warm years. The opposite occurred for streamflow identified in the UCR basin (Utah and Colorado), middle Atlantic (Missouri, Iowa and Illinois), southeast (coastal Louisiana/Alabama, Florida, Georgia, South Carolina, and North Carolina) and central (Virginia, Maryland, and central Pennsylvania) United States in that streamflow was significant during PDO warm years but were not significant during PDO cold years. On the basis of these results, significant differences in streamflow may result when comparing the UCR basin, middle Atlantic, northwest, central and northeast U.S. streamflow for PDO cold years and PDO warm years. This is most likely a result of nonlinear coupling of the interdecadal and interannual phenomena. On the basis of the phase of the interdecadal phenomenon, the response can be impacted such that the interannual signal is either enhanced or dampened.

4.2. Atlantic Ocean SSTs and Continental U.S. Streamflow (First Mode)

4.2.1. All Years

[29] For the all years analysis, Atlantic Ocean SSTs and continental U.S. streamflow resulted in squared covariance fractions of 53% for first mode, 21% for second

mode, and 7% for third mode, and a NSC value of 3.0%. Figure 3 represents heterogeneous correlation maps ($|r| > 0.29$) displaying significant Atlantic Ocean SST (left side) and continental U.S. streamflow regions (right side) for the first mode of SVD. The Atlantic Ocean SST heterogeneous correlation figure (Figure 3a) was determined by correlating the Atlantic Ocean SST values with the first temporal expansion series of continental U.S. streamflow while the continental U.S. streamflow heterogeneous correlation figure (Figure 3a) was determined by correlating the continental U.S. streamflow values with the first temporal expansion series of Atlantic Ocean SSTs. Atlantic Ocean SSTs (plus sign) were identified in the northern Atlantic Ocean and near the northern South American coast (Figure 3a) that correlated with continental U.S. streamflow.

[30] Streamflow regions (minus sign) were identified for the southwest, central, southeast and northeast U.S., while the northwest U.S. and the Florida peninsula regions display opposite (plus sign) responses (Figure 3a). The majority of streamflow stations (southwest, central, southeast, and northeast United States) experience decreased (increased) streamflow during a warming (cooling) of the northern Atlantic SST region while the opposite occurs for the northwest U.S. and the Florida peninsula regions.

[31] A spatially significant Atlantic Ocean SST region was identified in the northern Atlantic Ocean (Figure 3a). When correlating the AMO index with global SSTs, the highest correlations of the AMO index correspond to northern (north of the equator) Atlantic Ocean SSTs [Enfield *et al.*, 2001]. Rajagopalan *et al.* [2000] identified SSTs in the northern Atlantic Ocean that influenced continental U.S. drought. The AMO signal appears to be represented in the continental U.S. streamflow regions identified. Enfield *et al.* [2001] determined that the majority of the United States has above normal rainfall during the AMO cold phase, with the exception of the northwest U.S. and south Florida, which was positively correlated with the AMO (i.e., opposite response). This signal was represented in the streamflow regions identified in the all years (Atlantic Ocean SSTs) analysis (Figure 3a). The identification of the AMO signal was further verified when correlating the Atlantic Ocean SST SVD first temporal expansion series with the unsmoothed AMO and NAO indices for the same year and season. Correlation ($|r|$) values were 0.89 (AMO index and Atlantic Ocean SST SVD first temporal expansion series) and 0.33 (NAO index and Atlantic Ocean SST SVD first temporal expansion series), thus showing that the Atlantic Ocean SST SVD first temporal expansion series is strongly correlated with the AMO. Marshall *et al.* [2001] associated the SST tripole pattern with air-sea fluxes associated with the North Atlantic Oscillation (NAO) [Hurrell and Van Loon, 1995]. While the Atlantic Ocean SST regions identified in Figure 3a represent a tripole, the NAO signal was not strongly identified in the Atlantic Ocean SST SVD first temporal expansion series. Interestingly, Rajagopalan *et al.* [2000] identified drought regions (Montana, northern Georgia, western South Carolina, and the southwest/central United States) that differed from the streamflow regions identified. Rajagopalan *et al.* [2000] associated the drought regions with the NAO. This could be attributed to the use of different seasons, lead times, period of record, hydrologic

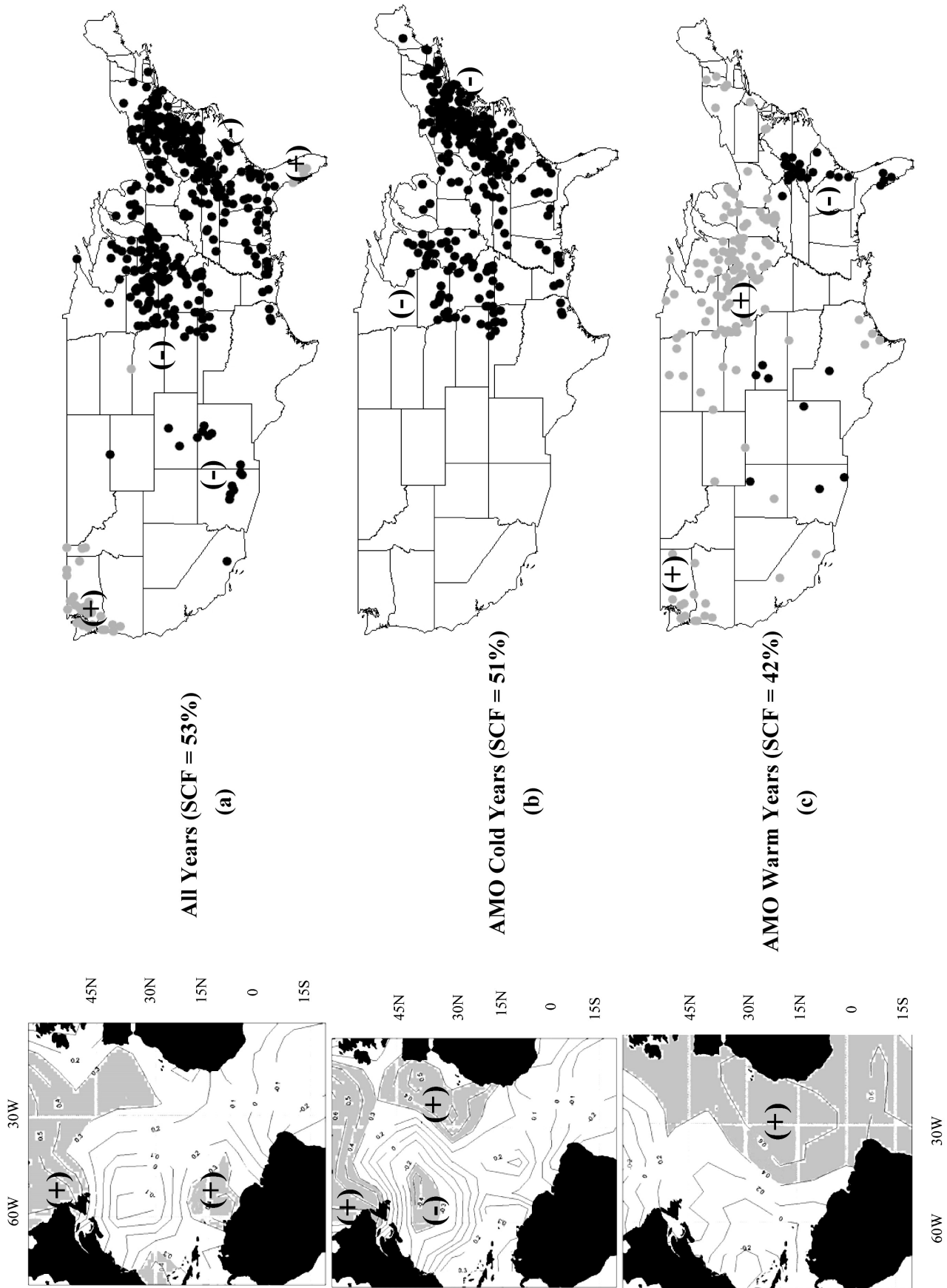


Figure 3

response variable (i.e., PDSI versus streamflow) and that global SSTs were evaluated.

[32] Next, the influence of the interdecadal AMO, based on the temporal phase (cold and warm), was examined in the following sections.

4.2.2. AMO Cold Years

[33] For the cold years analysis, Atlantic Ocean SSTs and continental U.S. streamflow resulted in squared covariance fractions of 51% for first mode, 17% for second mode, and 12% for third mode. When evaluating AMO cold years, Atlantic Ocean SSTs and continental U.S. streamflow regions ($|r| > 0.35$) were somewhat similar in spatial patterns when compared to the all years results. Atlantic Ocean SST regions (plus sign) were identified in the northern Atlantic and near the northwestern African coast while an SST region displaying opposite behavior (minus sign) was identified in the central Atlantic Ocean (Figure 3b). Streamflow regions (minus sign) were again identified in the central and northeast United States (Figure 3b), however, streamflow regions in the northwest, southwest and the Florida peninsula, previously identified in the all years results (Figure 3a), were no longer significant. This was consistent with the AMO warm years findings of *Enfield et al.* [2001], who identified the northwest and Florida peninsula. This may be attributed to the use of different seasons, lead times, period of record and hydrologic response variable (i.e., rainfall versus streamflow). Additionally, fewer stations were identified for the central and southeast United States when comparing AMO cold years (Figure 3b) and all years (Figure 3a).

4.2.3. AMO Warm Years

[34] For the warm years analysis, Atlantic Ocean SSTs and continental U.S. streamflow resulted in squared covariance fractions of 42% for first mode, 29% for second mode, and 8% for third mode. When evaluating AMO warm years, Atlantic Ocean SSTs and continental U.S. streamflow regions ($|r| > 0.43$) display large differences in the spatial patterns when compared to the all years (and AMO cold years) results. A spatially large SST region (plus sign) dominates the eastern Atlantic Ocean (Figure 3c). The SST region identified represented a distinct southeast shift in the apparent dominant Atlantic SST region when compared to the all years results (Figure 3a). Streamflow regions in the upper Mississippi River (UMR) and northwest U.S. (plus sign) behave similarly to the eastern Atlantic SST region such that increased (decreased) streamflow results from increased (decreased) SSTs. Streamflow stations on the Florida peninsula (minus sign) behave opposite to the eastern Atlantic SST region such that increased (decreased) streamflow results from decreased (increased) SSTs.

[35] The northwest United States and the Florida peninsula (Figure 3c) were identified as significant streamflow regions, unlike the AMO cold years (Figure 3b). Interestingly, the northwest United States (plus sign) and the Florida peninsula (minus sign) streamflow regions display opposite behavior, which differs from the all years results (Figure 3a). This was consistent with the AMO warm years

findings of *Enfield et al.* [2001]. A streamflow region (Figure 3c) in the UMR basin, previously not identified in Figures 3a or 3b, was found to be significant. Finally, streamflow regions in the Gulf of Mexico and northeast U.S. regions (Figure 3c), previously identified in the all years and AMO cold years, were no longer significant. When comparing AMO cold years and AMO warm years streamflow results, significant differences in streamflow may occur for the northwest, northeast, UMR basin and the Florida peninsula. *Rogers and Coleman* [2003] determined the streamflow response to the shift in phase of the AMO was apparent in the upper Mississippi River basin, the northern Rocky Mountain region and UCR basin. The most likely explanation of the varying results was the *Rogers and Coleman* [2003] study utilized core AMO warm (or cold) years and winter streamflow.

4.3. Temporal Expansions Series and Influenced Streamflow Regions

[36] The SVD of the cross-covariance matrix of SSTs and streamflow results in two matrices of singular vectors (i.e., SST matrix and streamflow matrix). The first mode of the SST matrix was projected onto the standardized SST anomalies matrix and the first mode of the streamflow matrix was projected onto the standardized streamflow anomalies matrix. This resulted in the first temporal expansion series for SSTs and streamflow, respectively. The first temporal expansions series were then normalized for the Pacific and Atlantic Ocean SSTs and continental U.S. streamflow for the all years analysis (Figure 4). The SVD SST first temporal expansion series was correlated with the continental U.S. streamflow first temporal expansion series and the correlation values were significant (Figure 4).

[37] It should be noted that the PDO and ENSO were highly correlated with the Pacific Ocean SVD SST first temporal expansion series and the AMO was highly correlated with the Atlantic Ocean SVD SST first temporal expansion series (see sections 4.1.1 and 4.2.1). The significant correlation results between the Pacific (and Atlantic Ocean) SVD SST first temporal expansion series and the continental U.S. streamflow first temporal expansion series display the distinct advantage of SVD in that the Pacific (and Atlantic) Ocean SVD SST first temporal expansion series considers and integrates the PDO and ENSO (and AMO) signals with other Pacific (Atlantic) Ocean influences. The significant correlations confirm that utilizing the ocean basin, as a whole, could result in improved streamflow predictability.

[38] Finally, Figures 2a and 3a (all years streamflow) were recalculated utilizing the Kendall correlation method, an alternative to the previously utilized linear correlation method. The Kendall correlation method is rank based, resistant to extreme values, and well suited for use with dependent variables (with a high degree of skewness) such as river discharge [*Maidment*, 1993]. Pacific Ocean streamflow stations were again identified in the northwest, southwest, central and southeast United States (Figure 4a).

Figure 3. Heterogeneous correlation figures for SVD (first mode) for previous year spring-summer season Atlantic Ocean SSTs and current water year U.S. streamflow for (a) all years, (b) AMO cold years, and (c) AMO warm years. Significant (>95%) SST regions were approximated by gray shading. Significant (>95%) negative (positive) streamflow stations were represented by black (gray) circles.

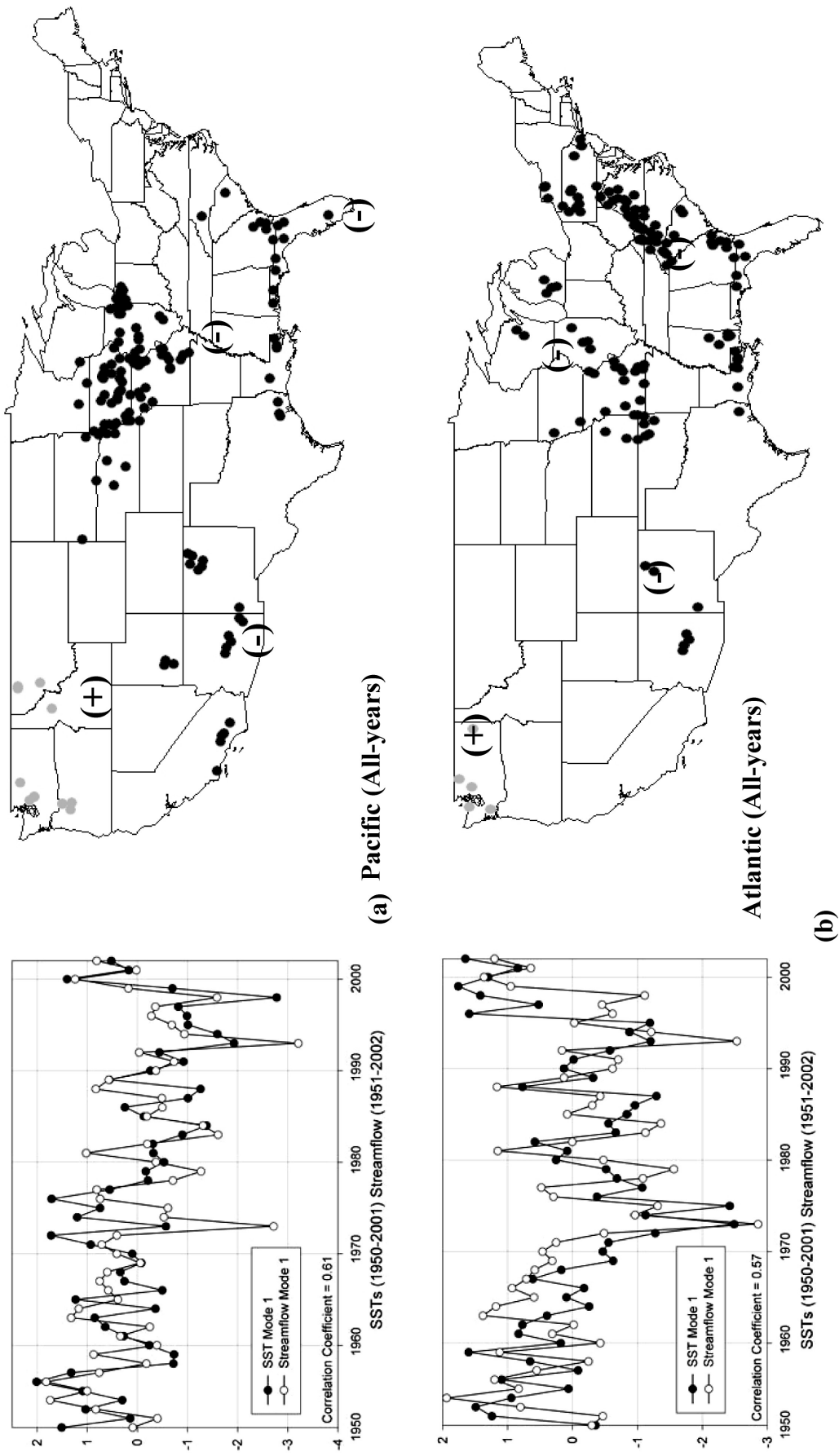


Figure 4. Temporal expansion series (standardized) for the first mode of SSTs and streamflow and streamflow stations (significant >95%) for Kendall's correlation coefficient) for (a) Pacific Ocean all years and (b) Atlantic Ocean all years. Significant (>95%) negative (positive) streamflow stations were represented by black (gray) circles.

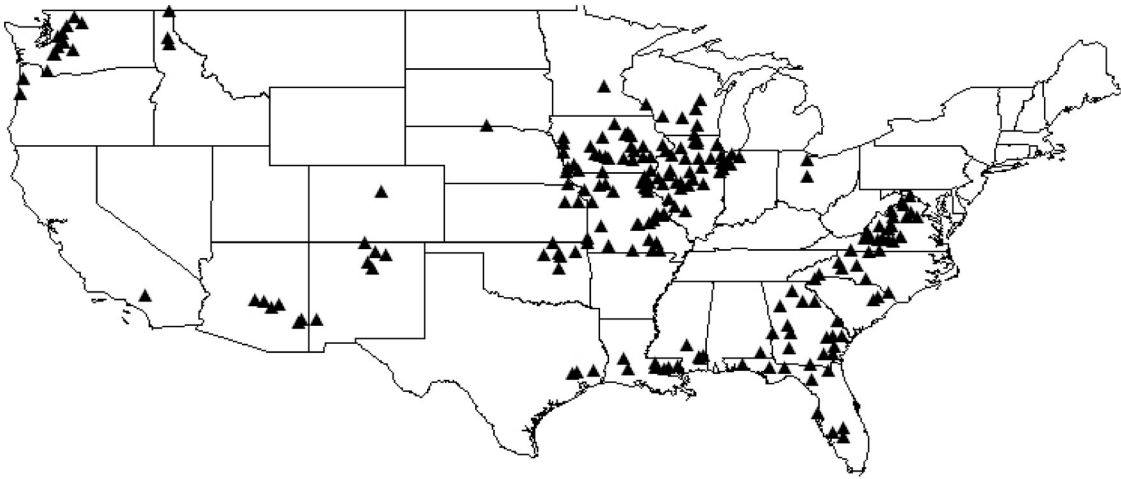


Figure 5. Streamflow stations (significant (>95%)) influenced by both Pacific Ocean and Atlantic Ocean SSTs from the all years analysis.

Atlantic Ocean streamflow stations were again identified in the northwest, southwest, central, southeast and middle Atlantic United States (Figure 4b). The Kendall correlation method results of the Pacific Ocean (Atlantic Ocean) compare favorably with Figure 2a (Figure 3a), with the primary difference being less streamflow stations were identified using the Kendall correlation method.

4.4. Streamflow Stations Influenced by Pacific and Atlantic Ocean SSTs

[39] Using the results from the all years analysis, 33% of the continental U.S. streamflow stations were influenced by both Pacific Ocean (Figure 2a) and Atlantic Ocean (Figure 3a) SSTs (Figure 5). This resulted in four continental U.S. streamflow regions being identified: northwest (Washington Cascade Mountains), southwest (southern Arizona and northern New Mexico), central (Missouri, Iowa and Illinois) and southeast (Florida, Georgia, southern Louisiana, western North Carolina and central Virginia). The NSC calculation for continental U.S. streamflow and, Pacific Ocean SSTs (3.6%) and Atlantic Ocean SSTs (3.0%) were close in value, revealing a similar level of influence when comparing the two ocean bodies. On the basis of the significant correlation results from Figures 2a and 3a, these regions may utilize the Pacific and Atlantic Ocean SVD SST first temporal expansion series for streamflow forecasting. This could result in improved long lead time forecasts of streamflow in these regions.

4.5. Detrended Oceanic SSTs and Continental U.S. Streamflow (First Mode)

[40] The sensitivity of the analysis provided above to inherent trends in the streamflow and SST data were tested in this section. For the all years period of record, the Pacific (and Atlantic) SSTs and continental U.S. streamflow data sets were detrended and the SVD analysis was performed. Pacific Ocean SSTs and continental U.S. streamflow

resulted in squared covariance fractions of 52% for first mode, 19% for second mode, and 8% for third mode, and a NSC value of 2.5%. (Figure 6a). The results were similar to the all years analysis of Pacific Ocean SSTs and continental U.S. streamflow (section 4.1.1) which resulted in squared covariance fractions of 57% for first mode, 13% for second mode, and 13% for third mode, and a NSC value of 3.6%. Additionally, the spatial patterns of Pacific Ocean SSTs and continental U.S. streamflow in Figure 6a were similar to those in Figure 2a.

[41] Atlantic Ocean SSTs and continental U.S. streamflow resulted in squared covariance fractions of 66% for first mode, 10% for second mode, and 7% for third mode, and a NSC value of 2.7%. (Figure 6b). The results were similar to the all years analysis of Atlantic Ocean SSTs and continental U.S. streamflow (section 4.2.1) which resulted in squared covariance fractions of 53% for first mode, 21% for second mode, and 7% for third mode, and a NSC value of 3.0%. Like the detrended Pacific Ocean results, the spatial patterns of Atlantic Ocean SSTs and continental U.S. streamflow in Figure 6b were similar to those in Figure 3a with the exception that peninsula Florida was no longer identified.

5. Conclusions

[42] An extended and interdecadal temporal evaluation of Pacific and Atlantic Ocean SST variability and continental U.S. streamflow variability was performed. When comparing the extended (i.e., all years) and the interdecadal phase (i.e., PDO/AMO warm or cold) results for both the Pacific and Atlantic Oceans, large differences in the spatial patterns occurs for SSTs and continental U.S. streamflow (Figures 2 and 3). The phase of the PDO impacts the spatial location of the Pacific Ocean tropical SST region. This resulted in a smaller spatial tropical SST region, centered near the equator, during PDO cold years and a large spatial SST

Figure 6. Heterogeneous correlation figures using detrended data sets for SVD (first mode) for previous year spring-summer season (a) Pacific Ocean SSTs and (b) Atlantic Ocean SSTs and current water year U.S. streamflow. Significant (>95%) SST regions were approximated by gray shading. Significant (>95%) negative (positive) streamflow stations were represented by black (gray) circles.

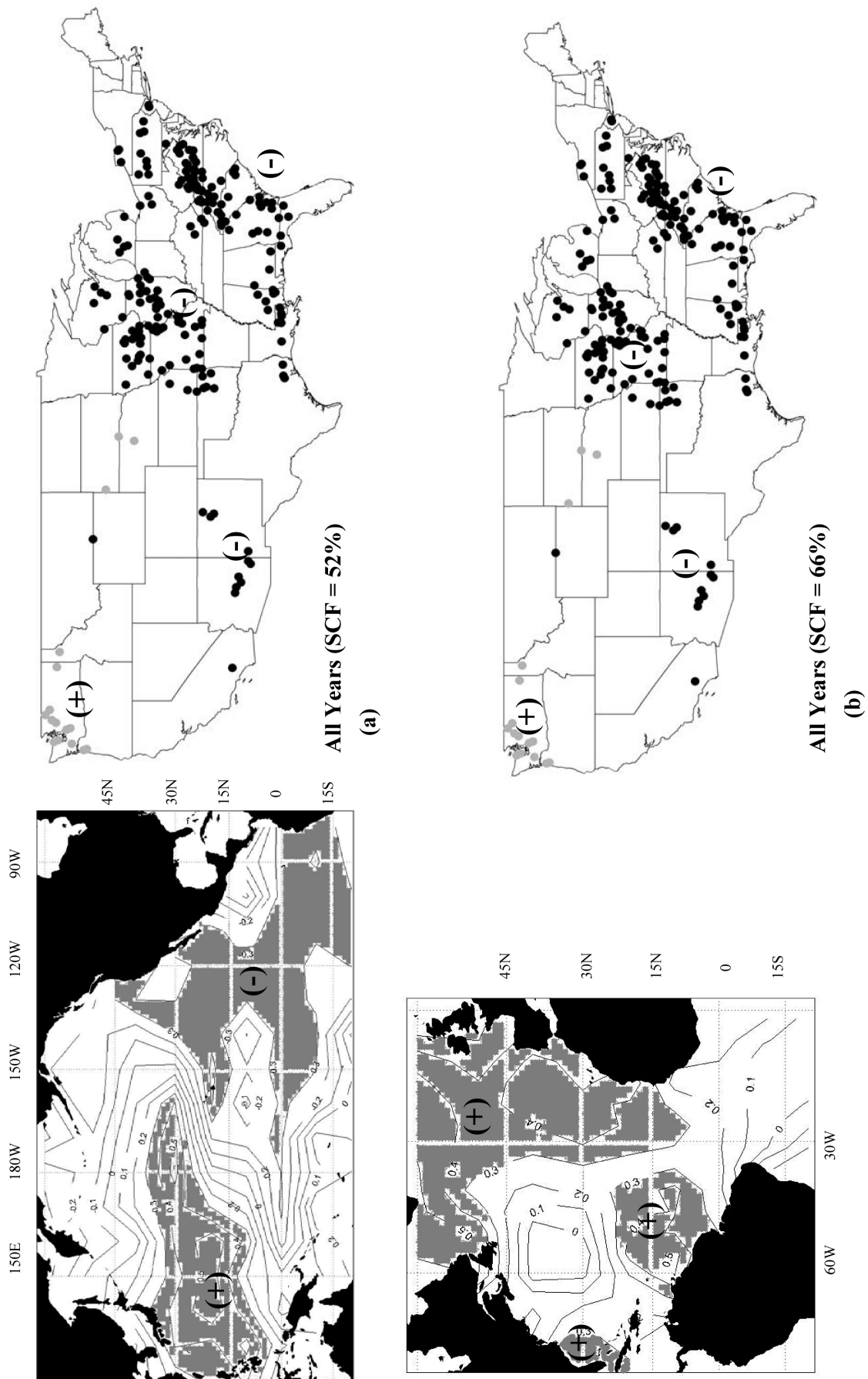


Figure 6

region in the eastern Pacific Ocean during PDO warm years. Interestingly, during PDO cold years, the well-defined tropical SST region resulted in significant continental U.S. streamflow stations being identified in established ENSO regions (i.e., northwest, southwest, southeast and northeast). While the ENSO signal was acknowledged for each (all years, PDO cold years and PDO warm years) analysis, tropical (ENSO) SST region was most defined during the PDO cold phase. The all years analysis was rerun using detrended data for both Pacific (and Atlantic) Ocean SSTs and continental U.S. streamflow. The spatial patterns were similar for the detrended all years analysis when compared to the original analysis.

[43] A significant SST region, displaying opposite behavior to the ENSO SST region, was identified in the north central Pacific Ocean. This region reported higher correlation values than the ENSO SST region, and, the identification of this region was also acknowledged by *Wang and Ting* [2000]. This may should be considered and further evaluated as a potential predictor of continental U.S. streamflow. The north central Pacific Ocean SST region also experienced differences in spatial patterns during cold and warm phases of the PDO.

[44] While *Rajagopalan et al.* [2000] identified the NAO signal in global SSTs and drought, the current research identified the AMO signal in Atlantic Ocean SSTs. Regions where streamflow was identified as being significant differed for AMO cold years and AMO warm years (northwest, northeast, UMR basin and the Florida peninsula), which could result in differences in yearly (water year) streamflow volume.

[45] A significant contribution of this research was the identification of streamflow predictors (i.e., Pacific and Atlantic Ocean SVD SST first temporal expansion series) that may improve long lead time forecasts of streamflow. The use of SVD integrates interdecadal (i.e., PDO and AMO) and interannual (i.e., ENSO) signals and incorporates all modes of oceanic SST variability. SVD eliminates any spatial and temporal bias by identifying new SST regions (i.e., north central Pacific Ocean) that were not predetermined. While the ENSO and PDO signals were acknowledged in the Pacific Ocean SVD SST first temporal expansion series and the AMO signal was acknowledged in the Atlantic Ocean SST first temporal expansion series, the integration of those signals (and other oceanic signals) resulted in significant correlations with streamflow. When correlating the PDO and Nino 3.4 indices with each (i.e., all 639) streamflow station, 2% and 8% of the streamflow stations achieved a correlation value exceeding 99% significance, respectively. When correlating the Pacific Ocean SVD first temporal expansion series with each streamflow station, 21% of the streamflow stations achieved a correlation value exceeding 99% significance, a significant improvement when compared to the PDO and Nino 3.4 indices. Additionally, when correlating the AMO index with each streamflow station, 11% of the streamflow stations achieved a correlation value exceeding 99% significance. However, when correlating the Atlantic Ocean SVD SST first temporal expansion series with each streamflow station, 15% of the streamflow stations achieved a correlation value exceeding 99% significance. Regions influenced by both Pacific and Atlantic Ocean SSTs (Figure 5) may have an

improved predictor (i.e., Pacific or Atlantic Ocean SVD SST first temporal expansion series) for long lead time streamflow forecasts. On the basis of the high correlation values of Pacific and Atlantic Ocean SVD SST first temporal expansion series with streamflow, future research may focus on utilizing SVD SST first temporal expansion series as predictors in streamflow forecasting models.

[46] **Acknowledgments.** This research is supported by the U.S. Geological Survey State Water Resources Research Program(s) of Nevada and Wyoming; National Science Foundation award CMS-0239334; the National Science Foundation, State of Nevada EPSCOR Graduate Fellowship; and the Wyoming Water Development Commission. The authors wish to thank the three anonymous reviewers for their helpful comments.

References

- Bretherton, C. S., C. Smith, and J. M. Wallace (1992), An intercomparison of methods for finding coupled patterns in climate data, *J. Clim.*, *5*, 541–560.
- Cayan, D. R., and D. H. Peterson (1989), The influence of North Pacific atmospheric circulation on streamflow in the west, in *Aspects of Climate Variability in the Pacific and the Western Americas*, *Geophys. Monogr. Ser.*, vol. 55, edited by D. H. Peterson, pp. 375–397, AGU, Washington, D. C.
- Cayan, D. R., and R. H. Webb (1992), El Niño/Southern Oscillation and streamflow in the western United States, in *El Niño: Historical and Paleoclimatic Aspects of the Southern Oscillation*, pp. 29–68, Cambridge Univ. Press, New York.
- Drosowsky, W., and L. Chambers (1998), Near global sea surface temperature anomalies as predictors of Australian seasonal rainfall, *Res. Rep. 65*, Bur. of Meteorol. Res. Cent., Melbourne, Victoria, Australia.
- Enfield, D. B., A. M. Mestas-Nuñez, and P. J. Trimble (2001), The Atlantic multidecadal oscillation and its relation to rainfall and river flows in the continental U. S., *Geophys. Res. Lett.*, *28*(10), 2077–2080.
- Gray, S. T., L. J. Graumlich, J. L. Betancourt, and G. T. Pederson (2004), A tree-ring based reconstruction of the Atlantic Multidecadal Oscillation since 1567 A. D., *Geophys. Res. Lett.*, *31*, L12205, doi:10.1029/2004GL019932.
- Hidalgo, H. G., and J. A. Dracup (2001), Evidence of the signature of North Pacific multidecadal processes on precipitation and streamflow variations in the upper Colorado River Basin, in paper presented at the 6th Biennial Conference of Research on the Colorado River Plateau, U.S. Geol. Surv., Phoenix, Ariz.
- Hurrell, J. W., and H. Van Loon (1995), Decadal variations in climate associated with the North Atlantic Oscillation, *Clim. Change*, *31*, 301–326.
- Kahya, E., and J. A. Dracup (1993), U.S. streamflow patterns in relation to the El Niño/Southern Oscillation, *Water Resour. Res.*, *29*(8), 2491–2503.
- Kahya, E., and J. A. Dracup (1994a), The influences of type 1 El Niño and La Niña events on streamflows in the Pacific southwest of the United States, *J. Clim.*, *7*(6), 965–976.
- Kahya, E., and J. A. Dracup (1994b), The relationships between U.S. Streamflow and La Niña events, *Water Resour. Res.*, *30*(7), 2133–2141.
- Kerr, R. A. (2000), A North Atlantic climate pacemaker for the centuries, *Science*, *228*, 1984–1986.
- Maidment, D. R. (1993), *Handbook of Hydrology*, McGraw-Hill, New York.
- Mantua, N. J. (2004), An overview of Pacific Decadal (climate) Variability impacts on hydroclimate and water resources management in the western US, *Eos Trans. AGU*, *85*(47), Fall Meet. Suppl., Abstract H24B-01.
- Mantua, N. J., and S. R. Hare (2002), The Pacific Decadal Oscillation, *J. Oceanogr.*, *59*(1), 35–44.
- Mantua, N. J., S. R. Hare, Y. Zhang, J. M. Wallace, and R. C. Francis (1997), A Pacific interdecadal climate oscillation with impacts on salmon production, *Bull. Am. Meteorol. Soc.*, *78*, 1069–1079.
- Marshall, J., Y. Kushnir, D. Battisti, P. Chang, A. Czaja, R. Dickson, J. Hurrell, M. McCartney, R. Saravanan, and M. Visbeck (2001), North Atlantic climate variability: Phenomena, impacts and mechanics, *Int. J. Clim.*, *21*, 1863–1898.
- Maurer, E. P., D. P. Lettenmaier, and N. J. Mantua (2004), Variability and potential sources of predictability of North American runoff, *Water Resour. Res.*, *40*, W09306, doi:10.1029/2003WR002789.

- McCabe, G. J., M. A. Palecki, and J. L. Betancourt (2004), Pacific and Atlantic ocean influences on multidecadal drought frequency in the United States, *Proc. Natl. Acad. Sci. U. S. A.*, *101*(12), 4136–4141.
- Newman, M., and P. D. Sardeshmukh (1995), A caveat concerning singular value decomposition, *J. Clim.*, *8*, 352–360.
- Nigam, S., M. Barlow, and E. H. Berbery (1999), Analysis links pacific variability to drought and streamflow in United States, *Eos Trans. AGU*, *80*(61), 621.
- Philander, S. G. (1990), *El Niño, La Niña and the Southern Oscillation*, Elsevier, New York.
- Rajagopalan, B., E. Cook, U. Lall, and B. K. Ray (2000), Spatiotemporal variability of ENSO and SST teleconnections to summer drought over the United States during the twentieth century, *J. Clim.*, *13*, 4244–4255.
- Rodriguez-Fonseca, B., and M. de Castro (2002), On the connection between winter anomalous precipitation in the Iberian Peninsula and north west Africa and the summer subtropical Atlantic sea surface temperature, *Geophys. Res. Lett.*, *29*(18), 1863, doi:10.1029/2001GL014421.
- Rogers, J. C., and J. S. M. Coleman (2003), Interactions between the Atlantic Multidecadal Oscillation, El Niño/La Niña, and the PNA in winter Mississippi Valley stream flow, *Geophys. Res. Lett.*, *30*(10), 1518, doi:10.1029/2003GL017216.
- Shabbar, A., and W. Skinner (2004), Summer drought patterns in Canada and the relationship to global sea surface temperatures, *J. Clim.*, *17*, 2866–2880.
- Smith, T. M., and R. W. Reynolds (2002), Extended reconstruction of global sea surface temperatures based on COADS data (1854–1997), *J. Clim.*, *16*, 1495–1510.
- Strang, G. (1998), *Introduction to Linear Algebra*, 2nd ed., Addison-Wesley, Reading, Mass.
- Trenberth, K. E. (1997), The definition of El Niño, *Bull. Am. Meteorol. Soc.*, *78*, 2271–2777.
- Tootle, G. A., T. C. Piechota, and A. K. Singh (2005), Coupled oceanic-atmospheric variability and U.S. streamflow, *Water Resour. Res.*, *41*, W12408, doi:10.1029/2005WR004381.
- Uvo, C. B., C. A. Repelli, S. E. Zebiak, and Y. Kushnir (1998), The relationships between tropical Pacific and Atlantic SST and northeast Brazil monthly precipitation, *J. Clim.*, *11*, 551–562.
- Wallace, J. M., D. S. Gutzler, and C. S. Bretheron (1992), Singular value decomposition of wintertime sea surface temperature and 500-mb height anomalies, *J. Clim.*, *5*, 561–576.
- Wallis, J. R., D. P. Lettenmaier, and E. F. Wood (1991), A daily hydroclimatological data set for the continental United States, *Water Resour. Res.*, *27*(7), 1657–1663.
- Wang, H., and M. Ting (2000), Covariabilities of winter U.S. precipitation and Pacific sea surface temperatures, *J. Clim.*, *13*, 3711–3719.

T. C. Piechota, Department of Civil and Environmental Engineering, University of Nevada, Las Vegas, 4505 Maryland Parkway, Box 454015, Las Vegas, NV 89154-4015, USA. (piechota@unlv.nevada.edu)

G. A. Tootle, Department of Civil and Architectural Engineering, University of Wyoming, 1000 E. University Avenue, Laramie, WY 82071-2000, USA. (tootleg@uwyo.edu)